3. CHARACTERIZATION OF GN SIGNALS

Signal characterization of the complex-baseband (CBB) gated-noise signals was accomplished via temporal, amplitude, and spectral analyses. Appendix C provides a theoretical evaluation of the corresponding amplitude and spectral characteristics of gated-noise signals in an ultra-wide transmission bandwidth. To evaluate the effects of band-limiting, the GN signals were measured with the vector signal analyzer (VSA) under optimal measurement conditions at the RF output of the vector signal generator (VSG) and under TOV operational conditions at the IF. Appendix D provides a description of the measurement setup, RF measurement results in various bandwidths, i.e., 36, 10, 1, and 0.1 MHz, and IF measurement results at the three different *SNR*s. Unless otherwise noted, analyses in this section use RF measurements sampled at f_s = 46.08 MSps (corresponding to VSA span = 36 MHz) and band-limited to B_{DTV} with the victim receiver RRC filter applied in post-measurement processing.

3.1. Temporal Analysis

Temporal characteristics of GN signals were evaluated with crossing statistics, which provide probabilities of the time a signal crosses an amplitude threshold and stays either above or below that threshold. Historically, this type of analysis has been used to study pulse statistics of noise [8], hence the terms pulse duration and pulse interval depicted in Figure 17. In this analysis of gated noise, their utility has been extended to the temporal statistics of noise bursts; accordingly, the terminology was changed to burst duration (*BD*) and burst interval (*BI*) as illustrated in Figure 18. For our purposes, the 10th percentile of the cumulative distribution function (*CDF*) of *BD* and *BI* using a threshold equal to -70 dBm was optimal for quantifying the effects of band-limiting on temporal characteristics of the GN signals.

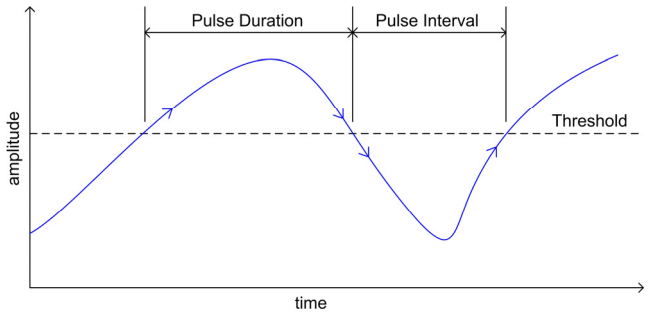

Figure 17. Illustration of pulse duration and pulse interval.

Table 3 summarizes the effects of band-limiting the GN signals to B_{DTV}. Note that *BD* and *BI* are given only when gating was resolved and the *CDF*s provided meaningful estimates of the band-limited on- and off-times, respectively. The band-limited fractional on-time, ζ_{DTV}, was computed as $BD/(BD + BI)$. As expected, band-limiting lengthened on-times, shortened off-times, and increased fractional on-times. Band-limited metrics approached the gating parameters only when τ_{on} and τ_{off} were significantly larger than $1/B_{DTV}$.

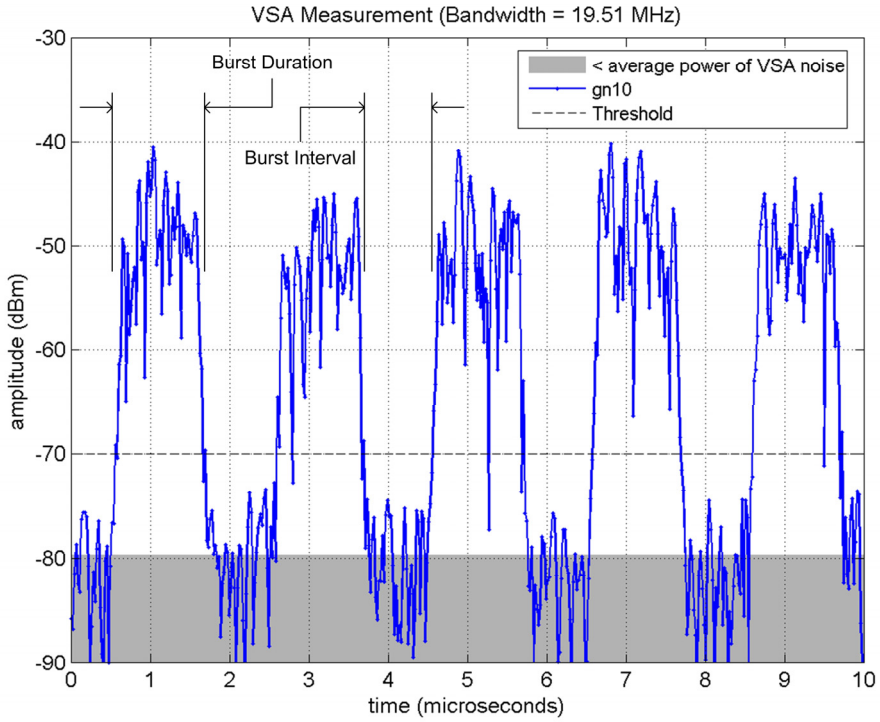

Figure 18. Illustration of burst duration and burst interval.

Table 3. Temporal Characteristics of GN Signals Band-Limited to B_{DTV}

GN	Gating Parameters			Band-Limited Metrics		
	τ_{on} (μs)	τ_{off} (μs)	ζ	BD (μs)	BI (μs)	ζ_{DTV}
01	∞	0.00	1.0000			1.00
02	0.01	0.01	0.5000			1.00
03	0.01	0.03	0.2500			1.00
04	0.01	0.07	0.1250			
05	0.01	0.15	0.0625			
06	0.10	0.10	0.5000			
07	0.10	0.30	0.2500	0.2	0.2	0.50
08	0.10	0.70	0.1250	0.2	0.6	0.25
09	0.10	1.50	0.0625	0.2	1.4	0.13
10	1.00	1.00	0.5000	1.1	0.9	0.55
11	1.00	3.00	0.2500	1.1	2.9	0.28
12	1.00	7.00	0.1250	1.1	6.9	0.14
13	1.00	15.00	0.0625	1.1	14.9	0.07
14	10.00	10.00	0.5000	10.1	9.9	0.51
15	10.00	30.00	0.2500	10.1	29.9	0.253
16	10.00	70.00	0.1250	10.1	69.9	0.126
17	10.00	150.00	0.0625	10.1	149.9	0.063

3.2. Amplitude Analysis

Random amplitudes of the gated-noise signals were characterized with the amplitude probability distribution, which describes the probability that signal amplitude exceeds a certain value. In this report, *APD*s are plotted on Rayleigh graphs where Rayleigh-distributed amplitudes of complex-Gaussian noise appear as a negatively-sloped, straight line. The sorting method, documented in Appendix D of Part 1, was used to estimate and plot *APD*s of 2^{17} = 131,072 samples that are free of correlation introduced by the measurement system and post-measurement band-limiting.

Figures 19 – 22 provide composite *APD* plots of the measured GN signals. Each plot represents a specific τ_{on}, and each curve within a plot represents a different ζ. Dashed lines represent the *APD* of the continuous-noise signal, GN-01. The upper bound of the shaded region is the average power of the VSA noise, approximately -79.7 dBm in B_{DTV}.

Band-limiting had profound effects on the *APD*s of the GN signals. If τ_{off} exceeded $1/B_{DTV}$ a step-like *APD* occurred, where higher amplitudes primarily corresponded to elongated on-times and lower amplitudes to the shortened off-times. This was most pronounced for GN-17 (τ_{on} = 10,000 ns, ζ = 0.0625). If τ_{off} was less than or comparable to $1/B_{DTV}$ a negatively-sloped, straight *APD* occurred, corresponding to Rayleigh-distributed amplitudes due to elongated noise bursts overlapping each other. This was most pronounced for GN-02 (τ_{on} = 10 ns, ζ = 0.50).

Peak-to-average ratio is a metric derived from the *APD* as illustrated in Figure 23 for GN-10. When interpreting *P/A* results, it is important to understand the bandwidth that peak and average powers were measured in, the duration or number of samples, and the statistical definition of peak in terms of percentage of samples. In this study, peak and average powers were measured in the same bandwidth to compute a single *P/A*. Also, peak power is defined as the amplitude exceeded 0.01% of the time, which corresponds to 13 of 131,072 samples. Figure C-2 shows how *P/A* changes with various peak definitions.

Table 4 summarizes measured *P/A* and *APD* characteristics for the band-limited GN signals. Also included are ultra-wide bandwidth limits to *P/A* derived in Section C.1. *APD* characteristics are labeled RAYL for Rayleigh-distributed amplitudes or RG for resolved gating, i.e., step-like *APD* whose amplitude falls below VSA average noise power at least 10% of the time.

Band-limiting affected *P/A*. If τ_{off} far exceeded $1/B_{DTV}$, then *P/A* approached the ultra-wide transmission bandwidth limit. If τ_{off} was less than $1/B_{DTV}$, then *P/A* approached the 9.6-dB value for Rayleigh-distributed amplitudes. When τ_{off} was between these extremes, *P/A* transitioned between the limits.

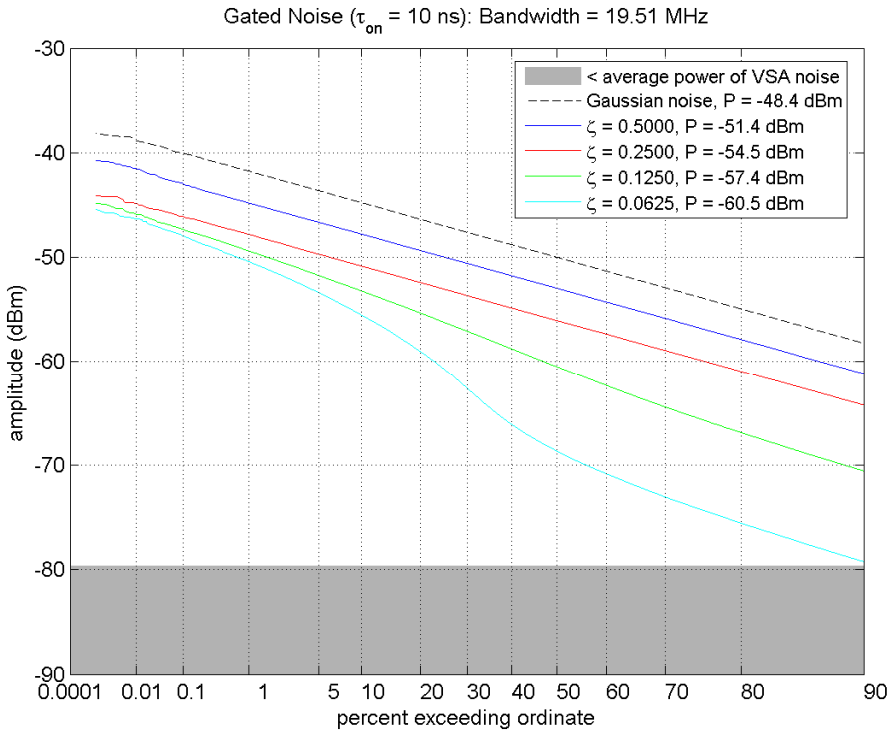

Figure 19. *APD*s of GN signals with τ_{on} = 10 ns band-limited to B_{DTV}.

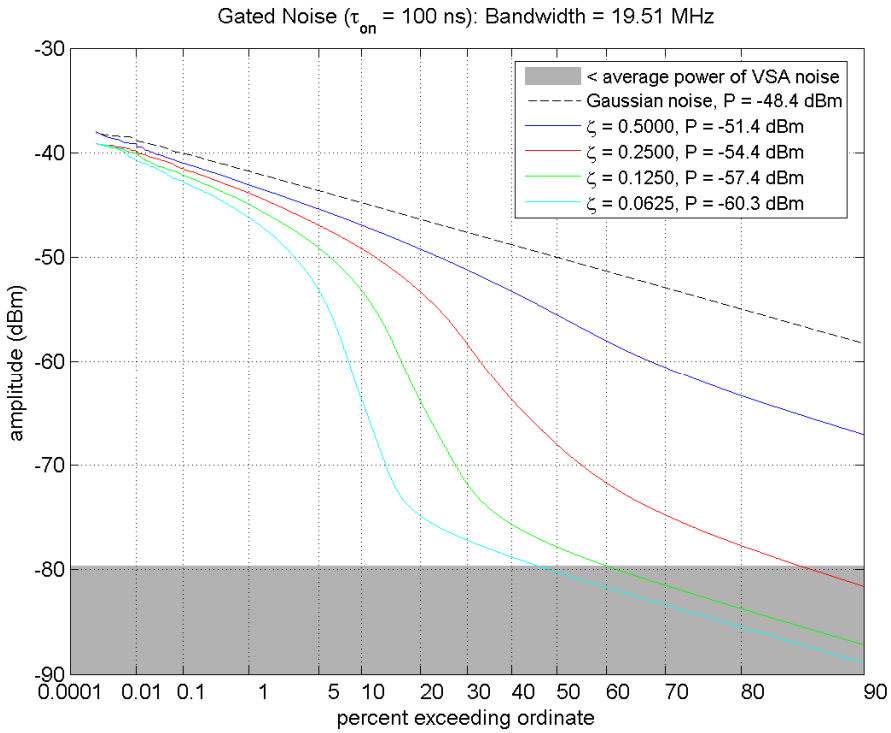

Figure 20. *APD*s of GN signals with τ_{on} = 100 ns band-limited to B_{DTV}.

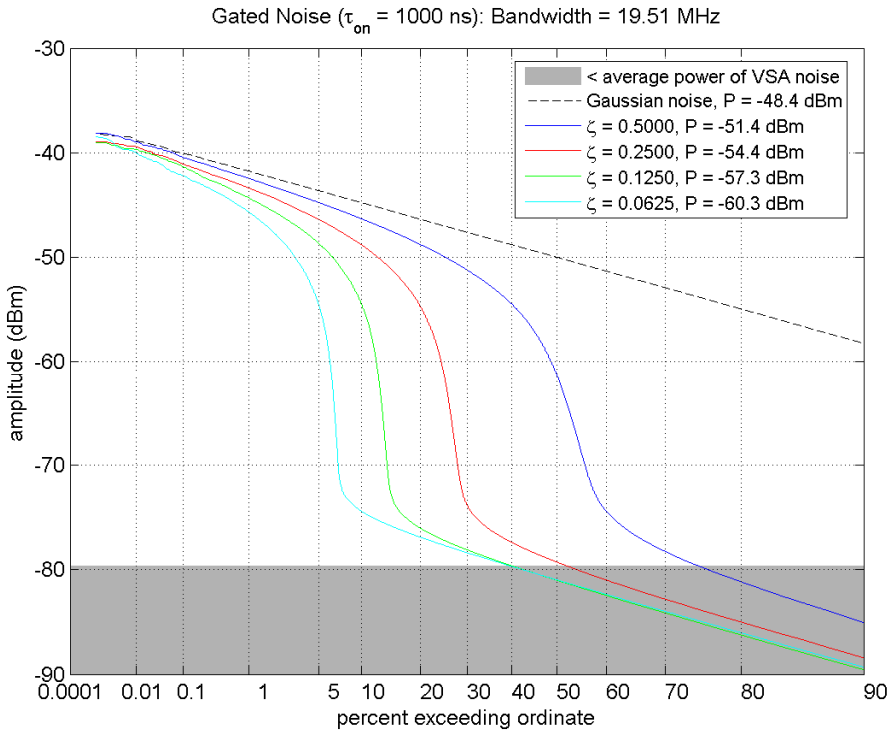

Figure 21. *APD*s of GN signals with τ_{on} = 1,000 ns band-limited to B_{DTV}.

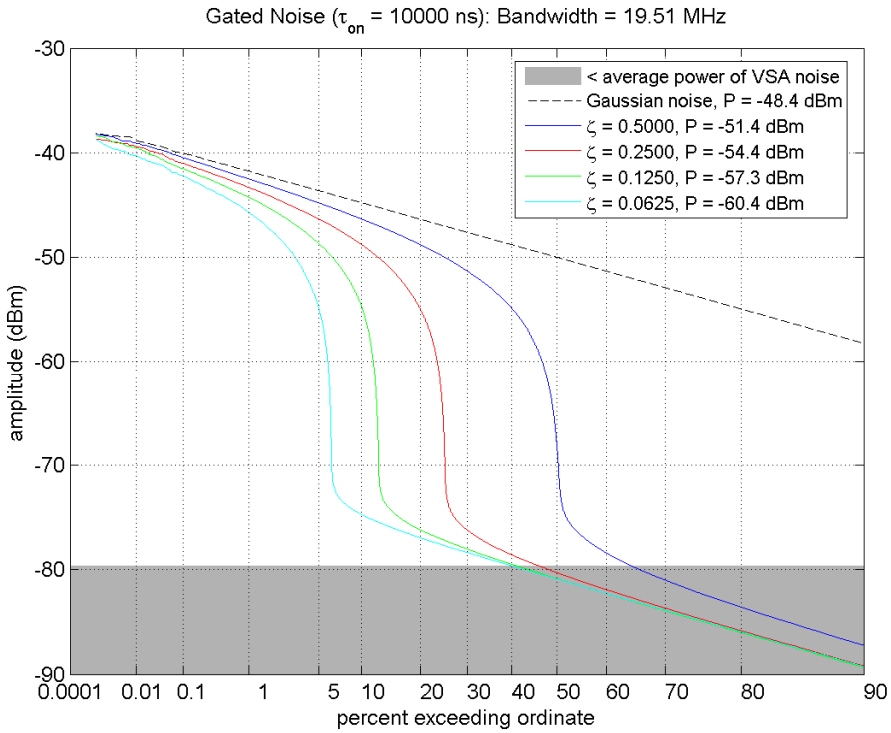

Figure 22. *APD*s of GN signals with τ_{on} = 10,000 ns band-limited to B_{DTV}.

Table 4. Amplitude Characteristics of GN Signals Band-Limited to B_{DTV}

GN	Ultra-wide Bandwidth Limits		Band-Limited Metrics	
	P/A (dB)	*APD*	*P/A* (dB)	*APD*
01	9.6	RAYL	9.6	RAYL
02	12.3	RG	9.9	RAYL
03	14.9	RG	9.7	RAYL
04	17.5	RG	11.5	
05	20.1	RG	14.2	
06	12.3	RG	12.2	
07	14.9	RG	14.6	RG
08	17.5	RG	17.3	RG
09	20.1	RG	19.6	RG
10	12.3	RG	12.4	RG
11	14.9	RG	15.0	RG
12	17.5	RG	17.6	RG
13	20.1	RG	20.3	RG
14	12.3	RG	12.3	RG
15	14.9	RG	15.1	RG
16	17.5	RG	17.8	RG
17	20.1	RG	20.1	RG

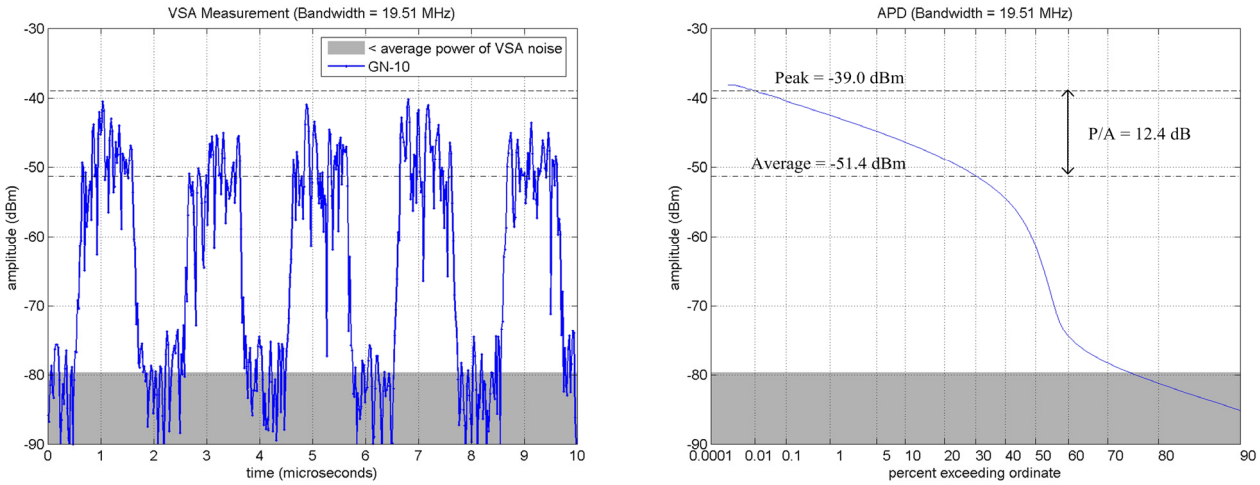

Figure 23. Illustration of *P/A* for GN-10 band-limited to B_{DTV}.

3.3. Spectral Analysis

Spectral characteristics of the gated-noise signals were characterized with the power spectral density, which represents the average power present per unit bandwidth as a function of frequency. Section C.2 provides a theoretical analysis of the *PSD* for gated Gaussian noise. In short, it can be considered to be constant over the bandwidth of interest.

Figures 24 – 27 provide *PSD*s of the GN signals over the entire VSA bandwidth, i.e., the victim receiver RRC filter was not applied to the data in post-measurement processing. *PSD*s were calculated by averaging squared spectrum magnitudes of rectangular-windowed, non-overlapping blocks of signal data. The periodic nature of the GN signals required that the block size be an integer multiple of the gating period. To have the same Δf for all *PSD*s, the block size must also be a common integer multiple of all gating periods. For the GN signals, these requirements were satisfied with a block size of 160 μs, which corresponds to Δf = 6.2 kHz. This allowed 500 blocks to be averaged, given the 4 million samples available in the acquired data sets.

The figures show that the power density of the gated signals decreased in proportion to ζ. In addition, the spectral spike at 0 Hz was due to VSG local-oscillator feed-through. The influence of the VSG local-oscillator feed-through to test results was discussed in Appendix C of Part 1.

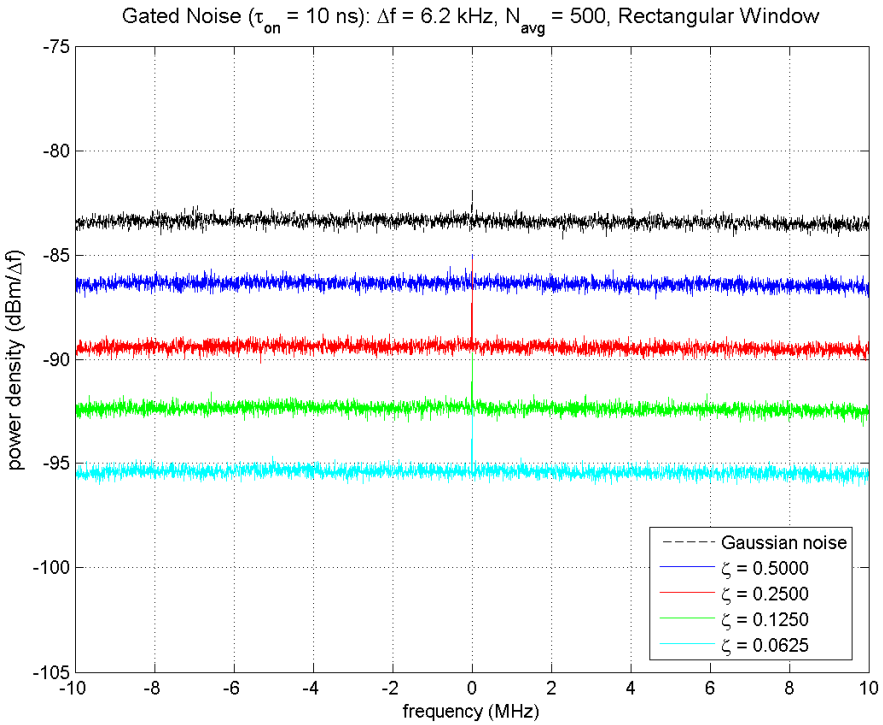

Figure 24. *PSD*s of GN signals with τ_{on} = 10 ns.

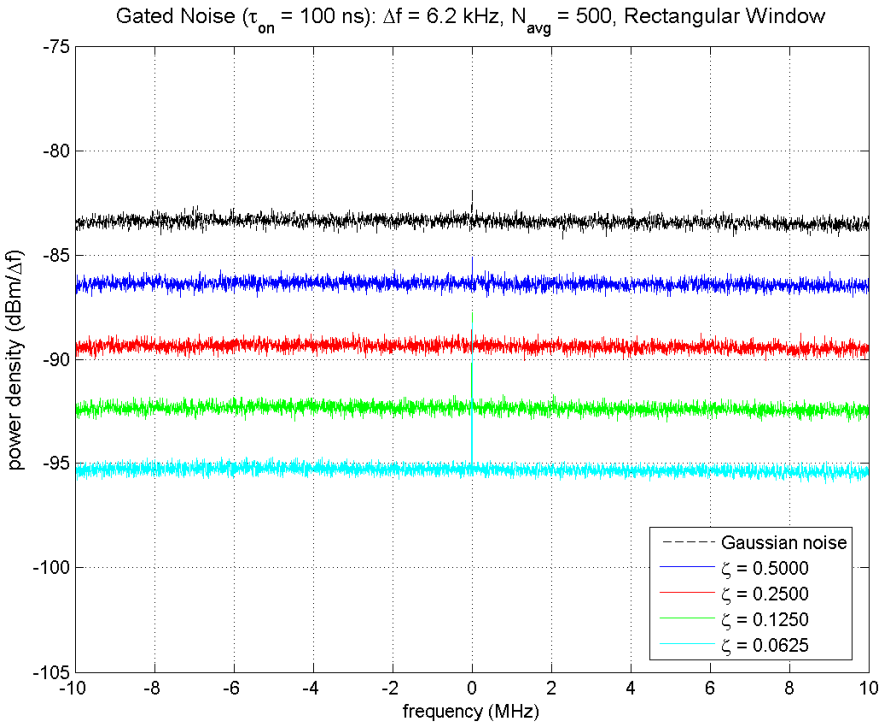

Figure 25. *PSD*s of GN signals with τ_{on} = 100 ns.

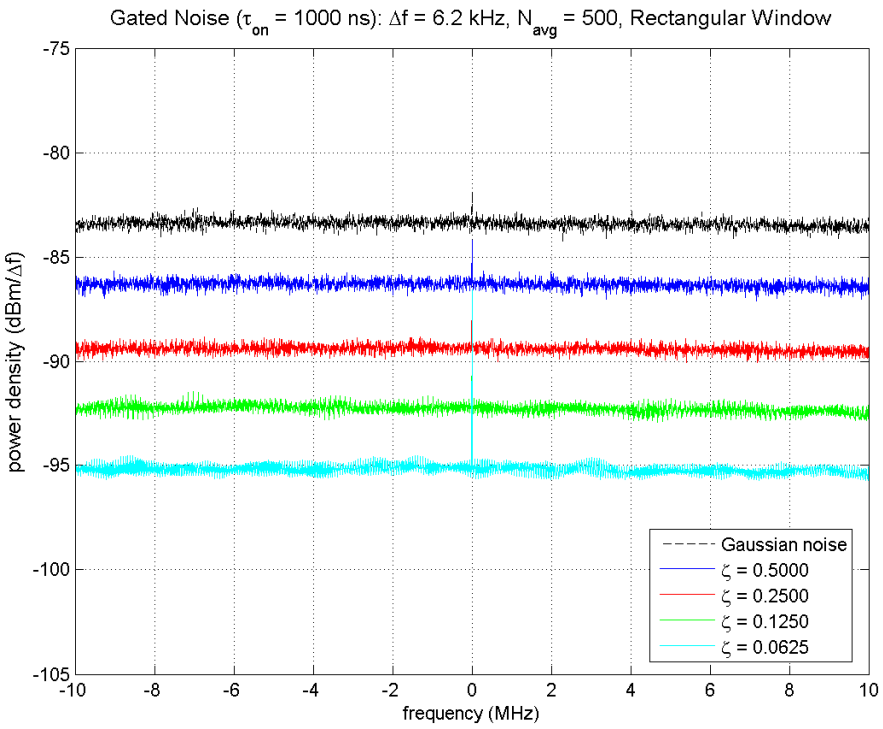

Figure 26. *PSD*s of GN signals with τ_{on} = 1,000 ns.

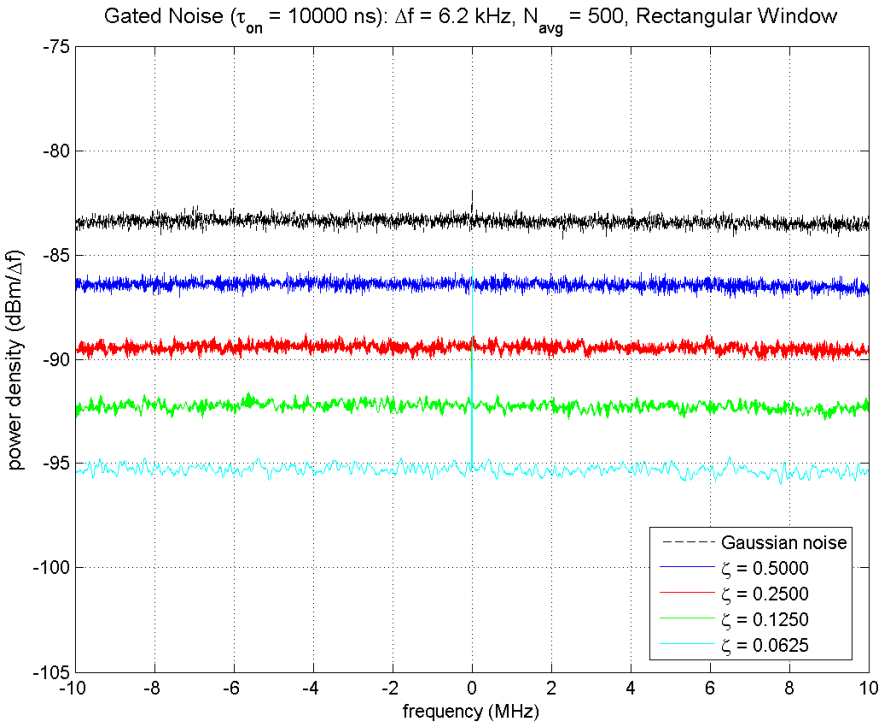

Figure 27. *PSD*s of GN signals with τ_{on} = 10,000 ns.